Silicon-Organic Hybrid MZI Modulator Generating OOK, BPSK and 8-ASK Signals for Up to 84 Gbit/s

R. Palmer,[1] L. Alloatti,[1] D. Korn,[1] P. C. Schindler,[1] R. Schmogrow,[1] W. Heni,[1]
S. Koenig,[1] J. Bolten,[2] T. Wahlbrink,[2] M. Waldow,[2] H. Yu,[3] W. Bogaerts,[3]
P. Verheyen,[4] G. Lepage,[4] M. Pantouvaki,[4] J. Van Campenhout,[4]
P. Absil,[4] R. Dinu,[5] W. Freude,[1] C. Koos,[1] and J. Leuthold[1,6]

[1]Institutes IPQ and IMT, Karlsruhe Institute of Technology (KIT), 76131 Karlsruhe, Germany
[2]AMO GmbH, 52074 Aachen, Germany
[3]Photonics Research Group, Department of Information Technology,
Ghent University—IMEC, 9000 Gent, Belgium
[4]IMEC vzw., 3001 Heverlee, Belgium
[5]GigOptix Inc., Switzerland and GigOptix, Bothell, WA 98011 USA
[6]Institute of Electromagnetic Fields (IFH), Swiss Federal Institute of Technology (ETH),
8006 Zurich, Switzerland

Abstract: We report on high-speed multilevel signal generation and arbitrary pulse shaping with silicon-organic hybrid (SOH) Mach–Zehnder interferometer (MZI) modulators. Pure phase modulation exploiting the linear electrooptic effect allows the generation of multiple modulations formats at highest speed such as 40-Gbit/s on–off-keying (OOK) and binary-phase-shift keying (BPSK) and 28-Gbd 4-ASK and 8-ASK with data rates up to 84 Gbit/s. Additionally, beside NRZ pulse shaping, for the first time, Nyquist pulse shaping with silicon modulators is demonstrated to enable multiplexing at highest spectral efficiency.

Index Terms: Electrooptic modulators, photonic integrated circuits.

1. Introduction

Silicon electrooptic modulators are key elements for photonic-electronic integration in telecommunications and optical interconnects. Devices capable of generating advanced modulation formats are of growing importance to increase bit rates while keeping symbol rates moderate and thus compliant with CMOS driver electronics. Commercial devices, relying on the linear electrooptic effect based on material platforms like $LiNbO_3$, so far have shown the best results for the generation of multilevel signals. For lack of a linear electrooptic coefficient, silicon modulators largely use free-carrier dispersion in forward-biased pin-junctions [1]–[3] or reverse-biased pn-junctions [4]–[9]. The latter concept enables higher modulation bandwidth [7] and has recently been used to demonstrate
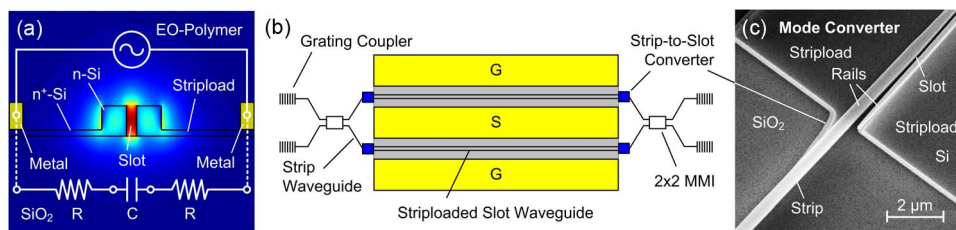
Fig. 1. (a) Schematic and simulated mode of a phase modulator. The optical field is confined in the 120 nm wide slot. The two rails of the slot waveguide are electrically connected to metal electrodes by 45 nm high n-doped (As, $1 \ldots 4 \times 10^{17}$ cm^{-3}) silicon strips (stripload). In this way the applied potential drops over the 120 nm wide slot. This results in a high electric field in the slot and in a high overlap between optical and electrical mode. (b) Schematic of the MZI modulator. The structure consists of two phase modulators, driven by a single coplanar waveguide (CPW). 2×2 MMI couplers are used as 3-dB power dividers. Grating couplers are used for fiber-chip coupling. (c) Scanning electron micrograph of a strip-to-slot converter used to couple access strip waveguides to the phase modulators.

50-Gbit/s quadrature-phase-shift keying (QPSK) with a single IQ modulator [10] and 112 Gbit/s with two IQ modulators and polarization multiplexing [11]. However, free-carrier dispersion leads to an intrinsic coupling of amplitude and phase modulation in all-silicon devices, which may render higher-order quadrature amplitude modulation (M-QAM, M > 4) challenging. In addition, so far reported nonresonant reverse-biased pn-modulators typically have voltage length products $V_\pi L$ not better than 10 Vmm and offer moderate extinction ratios (ERs) in the order of (3 to 8) dB at data rates above 20 Gbit/s [7], [9], while ERs exceeding 10 dB have been reported at lower data rates [12], [13]. A promising candidate to improve these results is silicon-organic hybrid (SOH) integration. SOH devices offer a linear electrooptic effect enabling pure phase modulation [14]. This allows for the generation of ideal amplitude and phase modulated signals in an Mach–Zehnder interferometer (MZI) configuration at moderate drive voltages [15], [16].

In this paper, we demonstrate generation of on–off-keying (OOK) and multilevel amplitude-shift-keying (ASK) signals using an SOH modulator. The device is operated at symbol rates up to 40 Gbd with 2 levels (OOK and binary-phase-shift keying (BPSK)] and at a symbol rate of 28 Gbd with 4 levels (4-ASK) and 8 levels (8-ASK). This is, to the best of our knowledge, the first demonstration of high-speed multilevel signal generation with a silicon-based modulator. With this device, we are able to generate a single polarization 8-ASK signal at a data rate of up to 84 Gbit/s—the highest data rate so far generated by an electrooptic MZI modulator on silicon. In addition, we demonstrate generation of Nyquist pulse-shaped BPSK and 4-ASK signals at a data rate of 21 Gbd.

2. SOH Modulator

SOH devices combine conventional silicon-on-insulator (SOI) waveguides with functional organic cladding materials [16]–[19]. The cross section of an SOH phase modulator is depicted in Fig. 1(a). It consists of two 240 nm wide and 220 nm high silicon rails separated by a 120 nm wide slot [20]. The waveguide is covered with an organic electrooptic cladding material. Field discontinuities at the slot sidewalls lead to strong confinement of the optical mode field within the electrooptic material in the slot. In this paper, we used the electrooptic polymer M3 of Gigoptix Inc. that has a nonlinear coefficient $r_{33} = 70$ pm/V if fully poled [21]. In addition, the rails are electrically connected to metal transmission lines by 45 nm thick n-doped silicon strips (stripload) such that the applied voltage drops predominantly across the 120 nm wide slot, resulting not only in a strong electric field but also in a large overlap with the optical mode. A $V_\pi L$ product of 2 Vmm is expected for this waveguide geometry if the electrooptic cladding is fully poled. The individual devices which are reported here have $V_\pi L$ products of (6–10) Vmm corresponding to nonlinear coefficients of (23–14) pm/V; therefore, poling can be improved. Other groups reached in-device nonlinear coefficients of up to 58 pm/V [22], underlining the potential of the approach to significantly reduce driving voltages.

The MZI modulator configuration is depicted in Fig. 1(b). It consists of a balanced MZI and two identical 1 mm long SOH phase modulators, Fig. 1(a). Two 2×2 multimode interference (MMI)
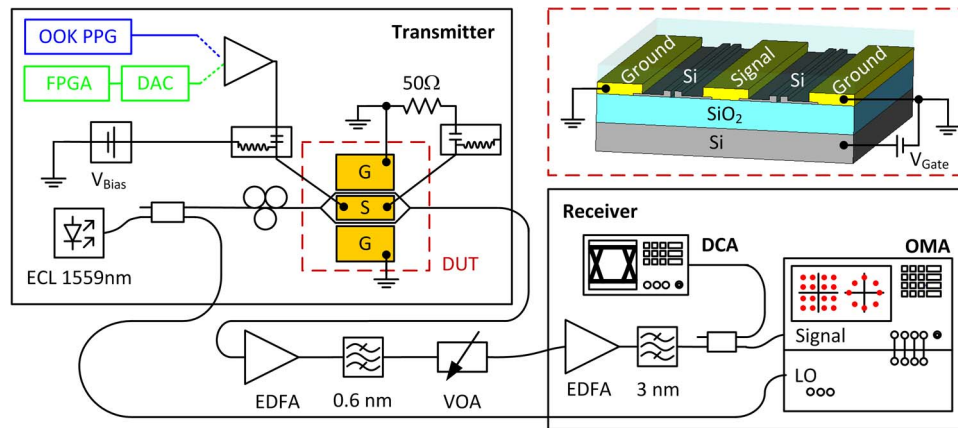
Fig. 2. Experimental setup. Two different signal generators are used. For generation of OOK and BPSK with symbol rates up to 40 Gbd a PPG (blue) is used. A second (software defined) signal generator (FPGA + DAC, green) is used to generate the M-ASK signals with data rates up to 28 Gbd. The signal is fed into the coplanar waveguide (CPW) of the modulator using a GSG Picoprobe and terminated by a second Picoprobe at the end of the modulator. CW light is coupled into the device after adjusting polarization. The same CW light serves as LO for the coherent detector. After amplification the signal is detected by a DCA and by a coherent receiver (OMA).

couplers are used for the MZI. The silicon waveguide structures were fabricated on an SOI wafer with a 220 nm thick silicon layer and 2 μm thick buried oxide. Grating couplers are used to couple light from a single-mode fiber to the silicon chip [23]. Fully etched strip waveguides are used as on-chip access waveguides. Efficient coupling between strip and strip-loaded slot waveguides is ensured by using logarithmically tapered mode converters [see Fig. 1(c)], as reported in [24]. A single coplanar transmission line is used to drive the push–pull MZI modulator. The two phase modulators have been poled with opposite polarities, referring to the signal electrode. The fiber-to-fiber loss is 20 dB with an on-chip loss of 9 dB in the C-band. We measure a loss of 0.2 dB per MMI, 0.02 dB per strip-to-slot converter, 1 dB loss for the access waveguides, and 7.5 dB loss in the 1 mm long active section. It should be noted that the loss of the striploaded slot waveguides in the active section increased only little after doping. Also, propagation losses of the waveguides remain the same when a PMMA cladding is exchanged with the EO-polymer M3 and are thus not dominated by absorption of the cladding. Therefore, the high propagation loss appears to be a fabrication issue. However, recently fabricated striploaded slot waveguides had a much lower loss below 1 dB/mm, indicating that the insertion loss of the devices can be significantly reduced by technology in future devices.

3. Data Transmission Setup

The experimental setup is shown in Fig. 2. Two different signal generators are set up to drive the modulator. A software-defined signal generator [field-programmable gate array (FPGA) + digital-to-analog converter (DAC), green] [25] is used to generate the 28 Gbd M-ASK signals based on a pseudorandom bit sequence (PRBS) of length $2^{11} - 1$. For the generation of OOK and BPSK signals with symbol rates of up to 40 Gbd, a second pseudorandom pattern generator is used with a bit sequence length of $2^{31} - 1$. The electrical signal is amplified to have a voltage swing of up to 6 V_{pp} for driving the device under test (DUT) via a GSG Picoprobe. A second Picoprobe with 50 Ω termination prevents reflections at the end of the device. Bias-Tees are used to adjust the operating point ($\varphi_{Bias} \propto V_{Bias}$) of the MZI modulator. In order to increase the conductivity of the silicon stripload [see Fig. 1(a)], a gate voltage has been applied between substrate and stripload (see Fig. 2). A detailed description of the effect of the gate voltage can be found in reference [14]. Light from an external cavity laser (ECL) at a wavelength of 1559 nm is coupled to the DUT. The input power is 8.5 dBm, and the polarization is adjusted to be quasi-TE on the chip. The same light source serves
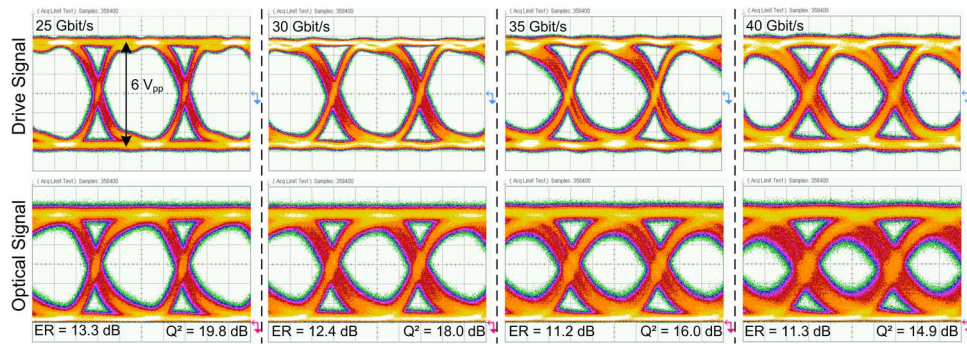
Fig. 3. OOK experiment. Recorded eye diagrams at various data rates. Measured ERs and Q^2-factors are depicted in the figure. The ER is above 11 dB at all data rates. The BER was measured. In the chosen measurement time no bit errors have been received for data rates up to 35 Gbit/s. At 40 Gbit/s the measured BER is 1×10^{-11}. A drive voltage of 6 V_{pp}, a gate field of 150 $V/\mu m$ and a PRBS of length $2^{31} - 1$ is used.

as local oscillator (LO) for the coherent receiver [optical modulation analyzer (OMA); Agilent Technologies N4391A]. After the DUT, the signal is amplified using two cascaded erbium-doped fiber amplifiers (EDFAs) and subsequently detected by a digital communications analyzer (DCA) and by a coherent receiver.

4. Experimental Results

In this paper, SOH modulators are used to generate NRZ-OOK signals with bit rates up to 40 Gbit/s, M-ASK signals with bit rates up to 84 Gbit/s, and M-ASK Nyquist pulse-shaped signals at a symbol rate of 21 Gbd. OOK experiments were performed with an MZI modulator fabricated by 193 nm deep UV lithography at IMEC, Belgium, with CMOS-like copper metallization and $V_\pi = 6$ V, while the coherent experiments were carried out using a second MZI modulator with identical design dimensions, fabricated by electron beam lithography at AMO, Germany, which has aluminum electrodes and $V_\pi = 10$ V.

4.1. Generation of OOK Signals

In the first experiment, the pseudorandom bit pattern generator (PPG; see Fig. 3, blue) is used to generate the electrical drive signal. The signal is amplified to have a voltage swing of 6 V_{pp}. Fig. 3 summarizes the measured eye diagrams and bit error ratios (BERs) at various data rates. At 25 Gbit/s and 40 Gbit/s, the ERs are 13.3 dB and 11.3 dB. No bit errors have been detected up to a data rate of 35 Gbit/s in the chosen measurement time indicating a BER below 1×10^{-12}. At 40 Gbit/s, a BER of 1×10^{-11} is measured.

4.2. Generation of M-ASK Signals

Single-polarization BPSK signals at symbol rates of 25 Gbd to 40 GBd are generated [see Fig. 4(a)–(c)], using the same pattern generator as before (see Fig. 2, blue) and adjusting the working point to the Null point. The optical signal was detected by the OMA and recorded with 80 GSamples/s. Digital signal processing and signal analysis are performed offline. An equalizer with a filter length of 55 symbols is used to compensate bandwidth limitations of the transmitter electronics, the OMA, and the SOH modulator. No bit errors have been measured in a set of 10 million recorded samples at these symbol rates, although a degradation of the error vector magnitude (EVM$_m$ [26], [27]) from 7.2% (25 Gbit/s) to 12.1% (40 Gbit/s) is observed.

Next, BPSK, 4-ASK, and 8-ASK signals are generated and received at a symbol rate of 28 Gbd by using a software-defined signal generator (see Fig. 2, green), which consists of an FPGA and a DAC [25]. The length of the bit sequence was $2^{11} - 1$. For operating the modulator in the linear regime, the drive voltage is reduced to 5.6 V_{pp}. The experimental results are depicted in Fig. 4(d)–(f).
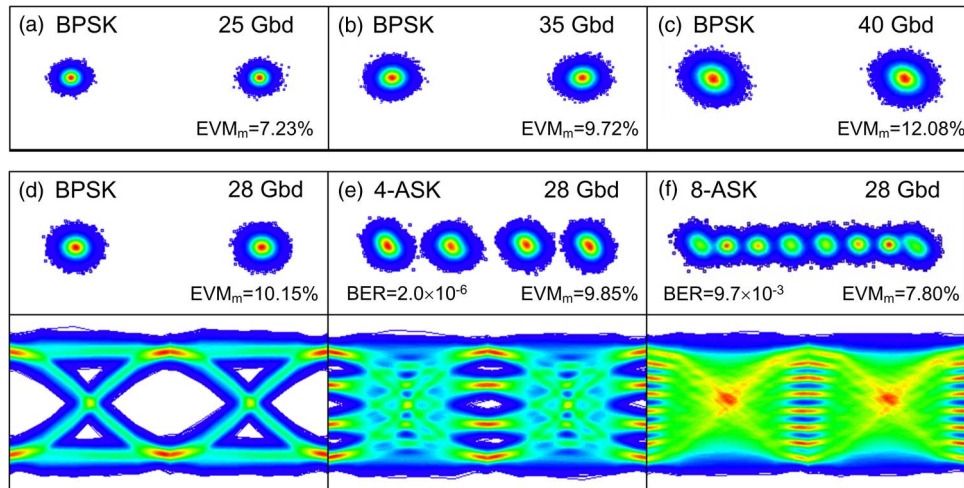
Fig. 4. Constellation diagrams and eye diagrams of the M-ASK signals. (a)–(c) BPSK signals at symbol rates of 25 Gbd (EVM$_m$ 7.2%), 35 Gbd (EVM$_m$ 9.7%) and 40 Gbd (EVM$_m$ 12.1%). No bit errors were detected. (d)–(f) M-ASK signals at a symbol rate of 28 Gbd. (d) BPSK. The EVM$_m$ is 10.2%. No bit errors were received. (e) 4-ASK. The EVM$_m$ is 9.9% with a BER of 2×10^{-6}. (f) 8-ASK. The EVM$_m$ is 7.8% and the BER was 9.7×10^{-3}. A drive voltage of 5.6 Vpp, a gate field of 150 V/μm and a PRBS of length $2^{11} - 1$ was used.

An EVM$_m$ of 10.2% is measured for BPSK[see Fig. 4(d)]. No errors are measured in a set of 3.5 million recorded bits. In the case of 4-ASK [see Fig. 4(e)], an EVM$_m$ of 9.9% and a BER of 2×10^{-6} are measured, well below the threshold of hard-decision FEC of 3×10^{-3}. Next, an 8-ASK signal is generated [see Fig. 4(f)], resulting in a gross data rate of 84 Gbit/s. An EVM$_m$ of 7.8% and a BER of 9.7×10^{-3} are measured, which are below the threshold of soft-decision FEC [28] (BER $= 1.9 \times 10^{-2}$) resulting in a net data rate of 67.2 Gbit/s (25% overhead). Taking also into account the 50-Ω termination of the transmission line, we estimate the energy consumption of the modulator to be 800 fJ/bit for the generation of 28-Gbd 8-ASK signals. We believe that improved poling procedures and device optimizations will allow to considerably increase the performance of the modulator: In the current device, an r$_{33}$ coefficient of 14 pm/V is obtained, measured at 5 GHz—a factor of 5 below the values obtained in polymer waveguides of the same material [21].

4.3. Generation of M-ASK Nyquist Pulse-Shaped Signals

Nyquist pulse shaping has been found to be a good candidate to increase spectral efficiency of optical communication systems [29], [30]. While, in wavelength division multiplex (WDM) systems, the spectrum of each carrier is usually infinitely broad, a finite rectangular spectrum with the bandwidth of the modulation frequency can be achieved by Nyquist pulse shaping, making guard intervals no longer necessary [31]. To do so, each bit is represented by a sinc-function in time domain, infinitely expanded in the ideal case. The Fourier transform of the sinc-function in time domain is a rectangular spectrum in frequency domain [see Fig. 5(a)]. The zero positions of the sinc-function are allocated in between two bit slots T$_s$. A Nyquist pulse-shaped PRBS of length $2^9 - 1$ is loaded to the software-defined signal generator. At a clock frequency of 28 GHz at the DAC, the signal is oversampled by a factor 4/3, resulting in a symbol rate of 21 Gbd [32]. The constellation diagrams for BPSK and 4-ASK are depicted in Fig. 5(b) and (c). EVMs of 18.2% and 16% are measured, respectively. Fig. 5(d) shows the optical spectrum of the 4-ASK signal. The expected rectangular shape is confirmed. The consumed optical bandwidth is 21 GHz and the ER is 20 dB.

5. Conclusion

We have experimentally demonstrated, for the first time, the generation of multilevel signals in SOH electrooptic modulators. Our device has been operated at a symbol rate of 28 GBd with up to
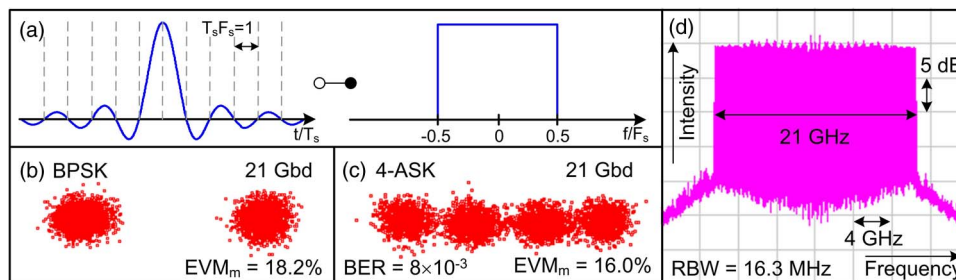
Fig. 5. Nyquist pulse shaping. (a) Nyquist pulse-shaped bit. The envelope of each bit is a sinc-function. The zero points of the sinc-functions are allocated between the bit slots T_s. The spectrum (Fourier transform) of a Nyquist pulse-shaped signal is a rectangular function. This allows for highly spectrally efficient WDM systems. (b), (c) Constellation diagrams of Nyquist BPSK and 4-ASK signals at a symbol rate of 21 Gbd. For BPSK an EVM_m of 18.2% and no bit errors have been measured. For 4-ASK an EVM_m of 16% is measured. The measured BER is 8×10^{-3}. (d) Spectrum of the Nyquist pulse-shaped signal. The rectangular shape of the spectrum is confirmed and an ER of 20 dB is measured.

8 symbols (8-ASK), resulting in a data rate of 84 Gbit/s. For BPSK and OOK, a symbol rate of 40 Gbd has been successfully demonstrated. This is, to the best of our knowledge, the highest symbol rate generated by an SOH MZI modulator, enabling the highest data rate generated by a single electrooptic MZI modulator on silicon. In addition, Nyquist pulse shaping has been performed for the first time by using a silicon modulator. We believe that our results are an important step toward 16-QAM and 64-QAM modulation using silicon devices in the near future.

Acknowledgment

References

[1] W. M. Green, M. J. Rooks, L. Sekaric, and Y. A. Vlasov, "Ultra-compact, low RF power, 10 Gb/s silicon Mach–Zehnder modulator," *Opt. Exp.*, vol. 15, no. 25, pp. 17 106–17 113, Dec. 2007.

[2] L. Chen, K. Preston, S. Manipatruni, and M. Lipson, "Integrated GHz silicon photonic interconnect with micrometer-scale modulators and detectors," *Opt. Exp.*, vol. 17, no. 17, pp. 15 248–15 256, Aug. 2009.

[3] S. Manipatruni, Q. Xu, B. Schmidt, J. Shakya, and M. Lipson, "High speed carrier injection 18 Gb/s silicon micro-ring electro-optic modulator," in *Proc. 20th Annu. Meet. IEEE LEOS*, Oct. 2007, pp. 537–538.

[4] P. Dong, S. Liao, D. Feng, H. Liang, D. Zheng, R. Shafiiha, C.-C. Kung, W. Qian, G. Li, X. Zheng, A. V. Krishnamoorthy, and M. Asghari, "Low V_{pp}, ultralow-energy, compact, high-speed silicon electro-optic modulator," *Opt. Exp.*, vol. 17, no. 25, pp. 22 484–22 490, Dec. 2009.

[5] L. Liao, A. Liu, J. Basak, H. Nguyen, M. Paniccia, D. Rubin, Y. Chetrit, R. Cohen, and N. Izhaky, "40 Gbit/s silicon optical modulator for high speed applications," *Electron. Lett.*, vol. 43, no. 22, Oct. 2007.

[6] F. Y. Gardes, D. J. Thomson, N. G. Emerson, and G. T. Reed, "40 Gb/s silicon photonics modulator for TE and TM polarisations," *Opt. Exp.*, vol. 19, no. 12, pp. 11 804–11 814, Jun. 2011.

[7] G. T. Reed, G. Mashanovich, F. Y. Garde, and D. J. Thomson, "Silicon optical modulators," *Nat. Photon.*, vol. 4, no. 8, pp. 518–526, Aug. 2010.

[8] D. J. Thomson, F. Y. Gardes, J.-M. Fedeli, S. Zlatanovic, Y. Hu, B. P. P. Kuo, E. Myslivets, N. Alic, S. Radic, G. Z. Mashanovich, and G. T. Reed, "50-Gb/s silicon optical modulator," *IEEE Photon. Technol. Lett.*, vol. 24, no. 4, pp. 234–236, Feb. 2012.

[9] T. Baehr-Jones, R. Ding, Y. Liu, A. Ayazi, T. Pinguet, N. C. Harris, M. Streshinsky, P. Lee, Y. Zhang, A. E.-J. Lim, T.-Y. Liow, S. H.-G. Teo, G. Q. Lo, and M. Hochberg, "Ultralow drive voltage silicon traveling-wave modulator," *Opt. Exp.*, vol. 20, no. 11, pp. 12 014–12 020, May 2012.

[10] P. Dong, L. Chen, C. Xie, L. L. Buhl, and Y.-K. Chen, "50-Gb/s silicon quadrature phase-shift keying modulator," *Opt. Exp.*, vol. 20, no. 19, pp. 21 181–21 186, Sep. 2012.

[11] P. Dong, C. Xie, L. Chen, L. L. Buhl, and Y.-K. Chen, "112-Gb/s monolithic DPM-QPSK modulator in silicon," presented at the Eur. Conf. Exhib. Optical Communication (ECOC), Amsterdam, The Netherlands, 2012, Paper Th.3.B.1.

[12] D. Thomson, F. Gardes, Y. Hu, G. Mashanovich, M. Fournier, P. Grosse, J. Fedeli, and G. Reed, "High contrast 40 Gbit/s optical modulation in silicon," *Opt. Exp.*, vol. 19, no. 12, pp. 11 507–11 516, Jun. 2011.

[13] K. Ogawa, K. Goi, Y. Tan, T. Liow, X. Tu, Q. Fang, G. Lo, and D. Kwong, "Silicon Mach–Zehnder modulator of extinction ratio beyond 10 dB at 10.0-12.5 Gbps," *Opt. Exp.*, vol. 19, no. 26, pp. B26–B31, Dec. 2011.

[14] L. Alloatti, D. Korn, R. Palmer, D. Hillerkuss, J. Li, A. Barklund, R. Dinu, J. Wieland, M. Fournier, J. Fedeli, H. Yu, W. Bogaerts, P. Dumon, R. Baets, C. Koos, W. Freude, and J. Leuthold, "42.7 Gbit/s electro-optic modulator in silicon technology," *Opt. Exp.*, vol. 19, no. 12, pp. 11 841–11 851, Jun. 2011.

[15] J.-M. Brosi, C. Koos, L. C. Andreani, M. Waldow, J. Leuthold, and W. Freude, "High-speed low-voltage electro-optic modulator with a polymer-infiltrated silicon photonic crystal waveguide," *Opt. Exp.*, vol. 16, no. 6, pp. 4177–4191, Mar. 2008.

[16] J. Leuthold, W. Freude, J.-M. Brosi, R. Baets, P. Dumon, I. Biaggio, M. L. Scimeca, F. Diederich, B. Frank, and C. Koos, "Silicon organic hybrid technology—A platform for practical nonlinear optics," *Proc. IEEE*, vol. 97, no. 7, pp. 1304–1316, Jul. 2009.

[17] C. Koos, P. Vorreau, T. Vallaitis, P. Dumon, W. Bogaerts, R. Baets, B. Esembeson, I. Biaggio, T. Michinobu, F. Diederich, W. Freude, and J. Leuthold, "All-optical high-speed signal processing with silicon-organic hybrid slot waveguides," *Nat. Photon.*, vol. 3, no. 4, pp. 216–219, Apr. 2009.

[18] J. H. Wuelbern, S. Prorok, J. Hampe, A. Petrov, M. Eich, J. Luo, A. K. Y. Jen, M. Jenett, and A. Jacob, "40 GHz electro-optic modulation in hybrid silicon-organic slotted photonic crystal waveguides," *Opt. Lett.*, vol. 35, no. 16, pp. 2753–2755, Aug. 2010.

[19] R. Ding, T. Baehr-Jones, W.-J. Kim, A. Spott, M. Fournier, J.-M. Fedeli, S. Huang, J. Luo, A. K.-Y. Jen, L. Dalton, and M. Hochberg, "Sub-volt silicon-organic electro-optic modulator with 500 MHz bandwidth," *J. Lightw. Technol.*, vol. 29, no. 8, pp. 1112–1117, Apr. 2011.

[20] V. R. Almeida, Q. F. Xu, C. A. Barrios, and M. Lipson, "Guiding and confining light in void nanostructure," *Opt. Lett.*, vol. 29, no. 11, pp. 1209–1211, Jun. 2004.

[21] D. Jin, "EO polymer modulators reliability study," in *Proc. SPIE*, vol. 7599, *Organic Photonic Materials and Devices XII*, 2010, p. 75 990H.

[22] X. Wang, C.-Y. Lin, S. Chakravarty, J. Luo, A. K.-Y. Jen, and R. T. Chen, "Effective in-device r33 of 735 pm/V on electro-optic polymer infiltrated silicon photonic crystal slot waveguides," *Opt. Lett.*, vol. 36, no. 6, pp. 882–884, Mar. 2011.

[23] D. Taillaert, F. Van Laere, M. Ayre, W. Bogaerts, D. Van Thourhout, P. Bienstman, and R. Baets, "Grating couplers for coupling between optical fibers and nanophotonic waveguides," *Jpn. J. Appl. Phys.*, vol. 45, no. 8A, pp. 6071–6077, Aug. 2006.

[24] R. Palmer, L. Alloatti, D. Korn, W. Heni, P. C. Schindler, J. Bolten, M. Karl, M. Waldow, T. Wahlbrink, W. Freude, C. Koos, and J. Leuthold, "Low-loss silicon strip-to-slot mode converters," *IEEE Photon. J.*, vol. 5, no. 1, p. 2 200 409, Feb. 2013.

[25] R. Schmogrow, D. Hillerkuss, M. Dreschmann, M. Huebner, M. Winter, J. Meyer, B. Nebendahl, C. Koos, J. Becker, W. Freude, and J. Leuthold, "Real-time software-defined multiformat transmitter generating 64QAM at 28 GBd," *IEEE Photon. Technol. Lett.*, vol. 22, no. 21, pp. 1601–1603, Nov. 2010.

[26] R. Schmogrow, B. Nebendahl, M. Winter, A. Josten, D. Hillerkuss, S. Koenig, J. Meyer, M. Dreschmann, M. Huebner, C. Koos, J. Becker, W. Freude, and J. Leuthold, "Error vector magnitude as a performance measure for advanced modulation formats," *IEEE Photon. Technol. Lett.*, vol. 24, no. 1, pp. 61–63, Jan. 2012.

[27] R. Schmogrow, B. Nebendahl, M. Winter, A. Josten, D. Hillerkuss, S. Koenig, J. Meyer, M. Dreschmann, M. Huebner, C. Koos, J. Becker, W. Freude, and J. Leuthold, "Corrections to 'Error vector magnitude as a performance measure for advanced modulation formats' [Jan 1, 2012 61-63]," *IEEE Photon. Technol. Lett.*, vol. 24, no. 23, p. 2198, Dec. 2012.

[28] T. Mizuochi, "Recent progress in forward error correction and its interplay with transmission impairments," *IEEE J. Sel. Topics Quantum Electron.*, vol. 12, no. 4, pp. 544–554, Jul./Aug. 2006.

[29] G. Bosco, V. Curri, A. Carena, P. Poggiolini, and F. Forghieri, "On the performance of Nyquist-WDM terabit superchannels based on PM-BPSK, PM-QPSK, PM-8QAM or PM-16QAM subcarriers," *J. Lightw. Technol.*, vol. 29, no. 1, pp. 53–61, Jan. 2011.

[30] R. Schmogrow, M. Winter, M. Meyer, D. Hillerkuss, S. Wolf, B. Baeuerle, A. Ludwig, B. Nebendahl, S. Ben-Ezra, J. Meyer, M. Dreschmann, M. Huebner, J. Becker, C. Koos, W. Freude, and J. Leuthold, "Real-time Nyquist pulse generation beyond 100 Gbit/s and its relation to OFDM," *Opt. Exp.*, vol. 20, no. 1, pp. 317–337, Jan. 2012.

[31] D. Hillerkuss, R. Schmogrow, M. Meyer, S. Wolf, M. Jordan, P. Kleinow, N. Lindenmann, P. C. Schindler, A. Melikyan, X. Yang, S. Ben-Ezra, B. Nebendahl, M. Dreschmann, J. Meyer, F. Parmigiani, P. Petropoulos, B. Resan, A. Oehler, K. Weingarten, L. Altenhain, T. Ellermeyer, M. Moeller, M. Huebner, J. Becker, C. Koos, W. Freude, and J. Leuthold, "Single-laser 32.5 Tbit/s Nyquist WDM transmission," *J. Opt. Commun. Netw.*, vol. 4, no. 10, pp. 715–723, Oct. 2012.

[32] R. Schmogrow, M. Meyer, P. Schindler, A. Josten, S. Ben-Ezra, C. Koos, W. Freude, and J. Leuthold, "252 Gbit/s real-time Nyquist pulse generation by reducing the oversampling factor to 1.33," presented at the Optical Fiber Communication Conf. (OFC), Anaheim, CA, USA, 2013, Paper OTu2I.1.